Non-Invasive Monitoring of Mode-Division Multiplexed Channels on a Silicon Photonic Chip

Stefano Grillanda, Francesco Morichetti, Nicola Peserico, Pietro Ciccarella, Andrea Annoni, Marco Carminati, and Andrea Melloni

I. Introduction

THE transmission of data channels on different orthogonal modes of a single fiber is currently envisioned as the primary path to scale the capacity of optical fiber networks and to address the continuous traffic growth [1]. This solution is typically implemented in systems using multimode and multicore fibers [2], and operating according to space-division multiplexing (SDM) and polarization-division multiplexing (PDM) schemes. In this scenario, several components such as mode converters, wavelength selective switches and amplifiers are needed in order to support fiber networks with multiple spatial paths [3].

Silicon (Si) photonics offers a versatile integrated platform to manipulate spatial modes and to carry out fundamental operations for SDM-PDM systems, such as space multiplexing/demultiplexing [4]–[7] and all-optical multiple-input-multiple-output mode unscrambling [4], potentially allowing to lower cost and reduce size with respect to bulk and free-space components. However, photonic integrated circuits (PICs) are sensitive to effects such as fabrication tolerances, temperature fluctuations, crosstalk etc., which are critical in Si and limit the operation of devices [8]. Therefore, it is fundamental to provide local monitoring and feedback control tools to Si devices in order to steer and hold their working point to the desired functionality, especially in circuits that perform complex operations on spatial modes [9].

Here, we show that the ContactLess Integrated Photonic Probe (CLIPP), that is a transparent photodetector for optical waveguides that we recently developed [10], [11], can monitor orthogonal modes propagating in a Si waveguide without affecting the quality of the transmitted signals (Section II). Also, we demonstrate that data channels that are trasmitted on a combination of orthogonal modes of the waveguide can be monitored simultaneously by the CLIPP, each one regardless of the presence of the others, and without affecting the overall performance of the system (Section III). Finally, the non-perturbative nature of the CLIPP suggests that no mode-dependent loss is added when monitoring different modes, thus inherently preserving their orthogonality, and proving its appeal for the realization and control of integrated spatial components, such as all-optical MIMO demultiplexers [4], [9].

II. The CLIPP

A. Concept and Readout

Fig. 1(a) shows a top-view photograph of the CLIPP, simply consisting of two metal electrodes deposited above the upper cladding of the Si waveguide. In the considered device, gold (Au) electrodes with size of 200 μm × 20 μm are placed at mutual distance of 100 μm. The 1 μm × 220 nm Si core, schematically shown in Fig. 1(b), is patterned by means of electron-beam lithography and reactive ion etching according to the process described in [12]. The silicon dioxide (SiO_2) top cladding is grown by plasma-enhanced chemical vapor deposition, while the Au electrodes are patterned with lift-off.

As shown in Fig. 1(b) the electrodes of the CLIPP are spaced by 1 μm from the Si core of the waveguide to avoid any significant metal loss. In fact, we estimate that for the considered waveguide the loss induced by the CLIPP electrodes is about 4×10^{-6} dB on the fundamental transverse electric mode (TE_0) of the waveguide and 3×10^{-2} dB on the fundamental transverse

Manuscript received October 6, 2014; revised November 28, 2014; accepted December 1, 2014. Date of publication December 3, 2014; date of current version March 4, 2015. This work was supported by the FP7-ICT European FET Project BBOI: Breaking the Barriers of Optical Integration (www.bboi.eu).

The authors are with the Dipartimento di Elettronica, Informazione e Bioingegneria, Politecnico di Milano, 20133 Milano, Italy (e-mail: stefano.grillanda@polimi.it; francesco.morichetti@polimi.it; nicola.peserico@mail.polimi.it; pietro.ciccarella@polimi.it; andrea.annoni@polimi.it; marco1.carminati@polimi.it; andrea.melloni@polimi.it).

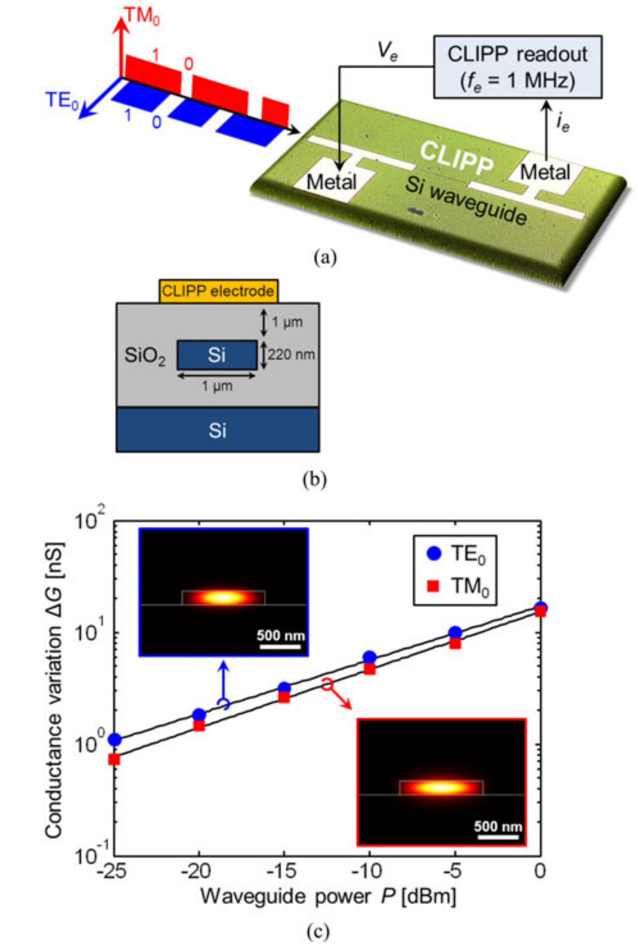

Fig. 1. On-chip monitoring of different orthogonal modes by using a CLIPP detector. (a) Top-view photograph of the CLIPP, that is composed simply of two metal electrodes, here spaced by 100 μm and with length 200 μm. (b) Cross-sectional schematic of the waveguide, with the CLIPP electrodes spaced by 1 μm from the Si core in order to avoid any appreciable loss. (c) Monitoring of two orthogonal modes, TE_0 and TM_0, as a function of the local waveguide power from -25 to 0 dBm when the CLIPP is driven with a sinusoidal voltage $V_e = 1$ V with frequency $f_e = 1$ MHz.

magnetic mode (TM_0). Although this loss is really negligible in practical applications, it can be further reduced by increasing the spacing between the metal and the Si core or by narrowing down the CLIPP electrodes, as in [11].

As extensively discussed in previous works [10], [11], the CLIPP monitors the optical intensity in the waveguide by measuring the light dependent change of the electric conductance G of the Si waveguide core. This effect is related to the photogeneration of free carriers at the waveguide core/cladding interfaces because of intrinsic surface state absorption (SSA) processes [13].

In order to measure remotely the Si conductance variation ΔG, that is without electrically contacting the Si core, the insulating top cladding needs to be bypassed. This means that, differently from conventional photodetectors, the CLIPP electrodes are AC-coupled to the Si waveguide core, this capacitive coupling being the key feature at the basis of the non-invasive nature of the CLIPP [10]. As sketched in Fig. 1(a), a sinusoidal voltage V_e at frequency f_e is applied to one of the CLIPP electrodes, while the current i_e at the other one is collected with a synchronous electrical detection architecture. The CLIPP readout requires a lock-in detection scheme [10] that can be integrated into CMOS electronics [11], the latter allowing to achieve better CLIPP performances and to simultaneously probe many CLIPPs embedded in complex photonic architectures.

The ability of the CLIPP to monitor different orthogonal modes is here demonstrated by using the first and third mode of the waveguide of Fig. 1(b), that are the TE_0 and TM_0 modes. Nevertheless, this concept is directly applicable to optical signals transmitted on orthogonal modes and same state of polarization, yet at the only price of adequately exciting them within the PIC. Fig. 1(c) shows the conductance variation measured by the CLIPP as a function of the local waveguide power P from -25 dBm to 0 dBm on both TE_0 (blue circles) and TM_0 (red squares) modes, whose intensity profiles at the wavelength of 1550 nm are reported in the inset of the figure.

The $\Delta G - P$ curves of the TE and TM polarized modes are almost overlapped, meaning that the CLIPP has a similar sensitivity on both polarizations. For a given density of surface states, that depends on the quality of the Si/SiO_2 interface, the density of the photogenerated carriers is related to the overlap of the optical mode with the waveguide boundary, that for the considered modes is comparable. In strongly multimode waveguides, where different modes typically exhibit different confinement within the waveguide core, the CLIPP sensitivity may substantially be different for the different modes. Nevertheless, the approach described in this work can still be used, provided that the CLIPP response is suitably calibrated on each mode.

B. Non-Perturbative Behavior

In a previous work we demonstrated that the CLIPP monitor introduces on the optical field a negligible phase perturbation, amounting to about 0.2 mrad (corresponding to an effective index variation of about 0.2 ppm) [10], this disturbance being much lower than the residual temperature fluctuations of thermally stabilized chips. Although this perturbation is negligible even in high-quality-factor resonators [10] or when tuning and feedback controlling Si PICs [11], it is fundamental to establish whether it has an impact on the quality of modulated signals transmitted through the waveguide.

To this aim we injected in the waveguide a 10 Gbit/s on-off keying (OOK) signal ($2^{31} - 1$ pseudorandom bit sequence) and then measured the system performances at the output of the waveguide. In this experiment, the field at the input of the waveguide is TE polarized, but the same results were achieved for TM polarized light. Figs. 2(a)–(b) report the eye diagrams measured respectively when the CLIPP is off ($V_e = 0$ V) and then switched on ($V_e = 1$ V), showing no appreciable evidence of disturbance added by the CLIPP. This is confirmed by the bit-error-rate (BER) measurements shown in Fig. 2(c). Blue circles report the BER of the bare Si waveguide when the CLIPP is off ($V_e = 0$ V), providing a benchmark for CLIPP performance evaluation. Then, as the CLIPP is turned on to monitor the signal (red squares, $V_e = 1$ V), no appreciable power penalty is observed. Since the sensitivity of the CLIPP increases with the applied read-out voltage [11], yet at the price of a linearly

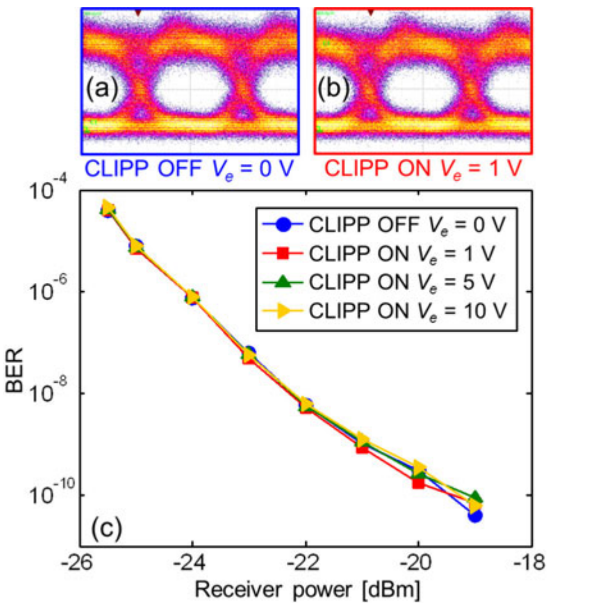

Fig. 2. No appreciable penalty is added by the CLIPP when monitoring a signal transmitted through the Si waveguide. Eye diagram of a 10 Gbit/s OOK signal measured at the output of the waveguide (a) when the CLIPP is off ($V_e = 0$ V) and (b) when is switched on ($V_e = 1$ V). (c) BER performance at the output of the waveguide when the CLIPP is off (blue circles) and then driven with increasing voltage from 1 to 10 V (red squares, green and yellow triangles).

increasing perturbation [10], we explored the BER performance at higher V_e. Results show no additional penalty when the voltage V_e is increased to 5 and 10 V [respectively green and yellow triangles in Fig. 2(c)].

III. Monitoring of Mode-Multiplexed Channels

Recently we have shown that the CLIPP can monitor and identify simultaneously and independently channels placed on different wavelengths by using weak pilot tones to label and discriminate each signal [11]. Here, we extend this concept to channels that are multiplexed on different modes of the waveguide. To this aim, we utilize the TE_0 and TM_0 modes considered in Section II, yet this application can be extended directly to a larger number of modes with arbitrary states of polarization.

A. Experimental Setup

Fig. 3 shows a schematic of the experimental setup used to multiplex and demultiplex the two channels on the TE_0 and TM_0 modes, and to monitor them on-chip with the CLIPP. A 10 Gbit/s OOK signal with wavelength 1558.18 nm and $2^{31} - 1$ pseudo-random bit sequence is equally splitted in two fiber optic paths. A weak pilot tone, with modulation depth $\delta = 4\%$, is added to each of the channels by means of $LiNbO_3$ Mach–Zehnder modulators. The two modulation tones have frequencies $f_1 = 10$ kHz and $f_2 = 17$ kHz respectively. On one of the paths a fiber coil is included to decorrelate the two channels, which are combined with a 50% fiber coupler and then transmitted through the Si chip. Light is coupled to and from the waveguide by means of lensed fibers. Polarization controllers (PC) are utilized to properly adjust the state of polarization of the signals on each path and at the input of the Si waveguide. The measurement setup is calibrated with a free-space polarizer to ensure that light on TE (TM) polarization of the fiber excites only TE (TM) polarized modes on the Si waveguide. Erbium-doped fiber amplifiers (EDFAs) and variable optical attenuators (VOAs) are used to finely control the intensity of the two channels that are launched into the Si waveguide.

On the receiver side, an EDFA and a VOA are utilized to compensate for the insertion loss of the chip, while a tunable bandpass filter with bandwidth 0.25 nm removes the amplified spontaneous emission noise generated by the EDFAs. Finally, the two channels (TE_0 and TM_0) are splitted with a fiber optic polarization beam splitter (PBS), and then sent to a BER tester and to a 20 GHz optical sampling oscilloscope to measure the system performance.

Finally, the electronics that manages the synchronous readout operations of the CLIPP applies also the pilot tones to the modulators. As anticipated in Section II, this electronic circuitry can be CMOS integrated [10], [11].

B. Experimental Results

Figs. 4(a)–(b) show the simultaneous temporal tracking of the two optical channels provided by the CLIPP. The two channels are discriminated by demodulating the CLIPP output current i_e at frequency $f_e + f_1 = 1.010$ MHz to monitor the signal on the TE_0 mode and at $f_e + f_2 = 1.017$ MHz to monitor the other one. Demodulation at frequency f_e provides information on the beating of the two channels, but would not allow the CLIPP to distinguish them, as in the case of wavelength-division multiplexed channels discussed in [11].

As a proof-of-concept experiment, we switch the power of the two channels on and off, and monitor the CLIPP signal versus time t. As shown in Fig. 4(a), when the channel placed on the TE_0 mode of the waveguide is off ($t < 10$ s), the CLIPP signal at frequency $f_e + f_1$ is zero. Then, as the light is switched on, it reaches the maximum value [Fig. 4(a)]. Fig. 4(b) shows that the same behavior can be observed on the TM_0 channel as well, when it is switched on ($t = 30$ s) and off ($t = 50$ s). Also, it is worth noticing that the monitoring of one channel does not affect the readout of the other one. In fact when probing the TE_0 (TM_0) mode as in Fig. 4(a) and (b), no appreciable evidence of the variations of the TM_0 (TE_0) mode is observed.

However, when using pilot tones to label and identify modulated signals it is fundamental to keep their intensity as low as possible, so that the performance of the overall system is not affected. To test the impact of these tones on our system we injected only one of the two channels in the Si waveguide with the CLIPP in the off state ($V_e = 0$ V) and measured the BER performance at its output, as shown in Fig. 4(c). To provide a benchmark level, the BER is measured when no pilot tone ($\delta = 0\%$) is applied to the modulated signal (blue circles). Then, as the pilot tone is switched on ($\delta = 4\%$, red squares) the BER measurement shows that no significant penalty is added to the overall performance of the system, indicating that the tones

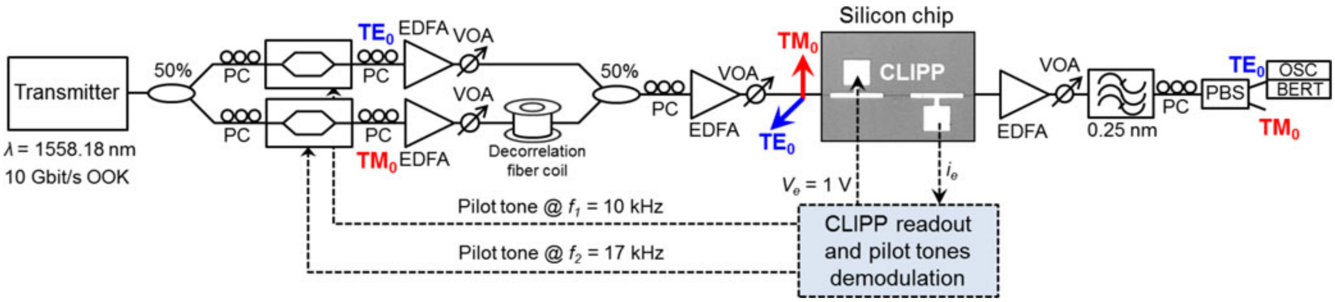

Fig. 3. Experimental setup utilized to multiplex and demultiplex the two data channels on the TE_0 and TM_0 modes of the waveguide, and to monitor them non-invasively with the CLIPP. Solid lines indicate optical fiber connections, whereas dashed lines indicate electrical connections.

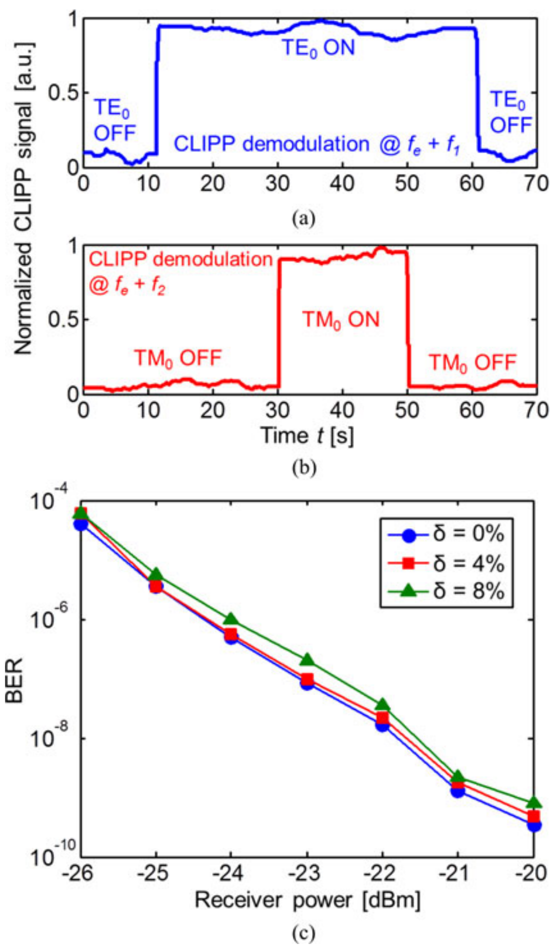

Fig. 4. Simultaneous CLIPP monitoring and discrimination of two mode-multiplexed channels transmitted through the Si chip. Readout of (a) the first channel placed on the TE_0 mode and of (b) the second channel placed on the TM_0 mode of the waveguide. In both cases the modulation depth of the pilot tones is $\delta = 4\%$ (both channels are simultaneously transmitted in the system). (c) BER measurements showing the non-perturbative behavior of the pilot tones up to a modulation depth $\delta = 4\%$. In this case only one channel is transmitted through the chip and the CLIPP is switched off.

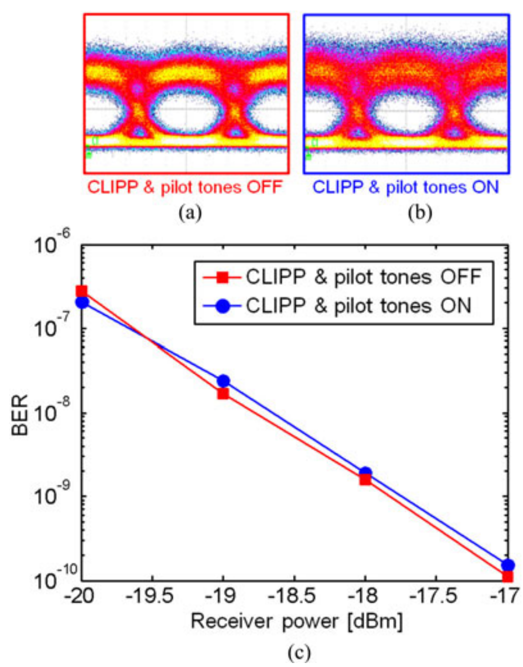

Fig. 5. Impact of the CLIPP monitoring on the quality of the mode-multiplexed channels (both signals are simultaneously transmitted through the system). Eye diagrams of the received TE_0 signal when (a) the CLIPP and the pilot tones are both off and (b) then switched on to monitor the two channels. (c) BER measurements when CLIPP and pilot tones are both off (red squares) and both on (blue circles). No appreciable penalty is observed. In these measurements, when channel monitoring is active the CLIPP voltage is $V_e = 1$ V and the modulation depth of the pilot tones is $\delta = 4\%$.

used in this experiment are non-invasive. Indeed, pilot tones with larger modulation depth were tested as well. For instance, green triangles indicate that, when the tone has a modulation depth $\delta = 8\%$, a penalty of less than 0.5 dB in the BER is observed across the entire dynamic range of the receiver, this value being within the estimated error bar of our setup. Larger tones, although providing a better CLIPP sensitivity, would significantly affect the system performance, and therefore should be avoided in practical applications.

Finally, we test the performance of the entire system of Fig. 3 to investigate whether the use of the CLIPP and pilot tones introduces any disturbance to the mode-multiplexed channels. Fig. 5 shows the eye diagrams of the received TE_0 signal when the CLIPP and the pilot tones are both off [see Fig. 5(a)] and then switched on to monitor the two channels [see Fig. 5(b)] (in this case both channels are simultaneously transmitted through the system). The eye aperture remains essentially the same in the two cases, proving that no significant signal degradation is caused by the CLIPP and the pilot tones. This is confirmed by the BER measurements of Fig. 5(c), where no appreciable penalty is introduced by the CLIPP and by the pilot tones across the whole dynamic range of the receiver. The same results are obtained when the orthogonally polarized TM_0 channel is detected.

IV. Conclusion

We have demonstrated that the CLIPP detector can be suitably used to monitor non-invasively data channels that are transmitted on a combination of orthogonal modes of a Si waveguide.

By applying a weakly modulated pilot tone to each signal, the CLIPP can discriminate and monitor simultaneously the light intensity of the different modes. BER measurements show that neither the addition of the pilot tone nor the CLIPP monitoring operations introduces any penalty to the system performance. Noteworthy, thanks to the transparent nature of the CLIPP the behavior of the different modes can be tracked in time without inducing any appreciable disturbance: no significant mode-dependent loss is added and orthogonality relations are preserved.

Finally, since the CLIPP monitors the average power of the transmitted channels, the proposed technique is directly applicable to any modulation format and bit rate. Also, in our experiments we utilized the first and third mode of a Si waveguide, that is the fundamental TE and fundamental TM mode, yet this approach can be scaled up to a larger number of modes with arbitrary state of polarization. Indeed, this indicates that the CLIPP is an appealing technology for the realization of Si photonic components for SDM-PDM systems, such as mode multiplexers and all-optical MIMO demultiplexers.

Acknowledgment

The authors thank A. Canciamilla and A. Cavaciuti from Cisco Systems for support with the BER measurements; M. Strain from the University of Strathclyde, M. Sorel and the staff of the J. Watt Nanofabrication Centre at Glasgow University for the fabrication of the Si photonic chip; G. Bellotti from Politecnico di Milano for support with the measurements; M. Sampietro from Politecnico di Milano for fruitful discussion.

References

[1] P. J. Winzer, "Making spatial multiplexing a reality," *Nat. Photon.*, vol. 8, no. 5, pp. 345–348, May 2014.

[2] D. J. Richardson, J. M. Fini, and L. E. Nelson, "Space-division multiplexing in optical fibres," *Nat. Photon.*, vol. 7, no. 5, pp. 354–362, May 2013.

[3] R. Ryf, "SDM components and MIMO experiments in multimode and multicore fibers," presented at the Eur. Conf. Opt. Commun., Cannes, France, 2014, Paper Th.2.1.1.

[4] N. K. Fontaine, C. R. Doerr, M. A. Mestre, R. Ryf, P. J. Winzer, L. L. Buhl, Y. Sun, X. Jiang, and R. Lingle, Jr., "Space-division multiplexing and all-optical MIMO demultiplexing using a photonic integrated circuit," presented at the Opt. Fiber Commun. Conf., Los Angeles, CA, USA, 2012, Paper PDP5B.1.

[5] T. Su, R. P. Scott, S. S. Djordjevic, N. K. Fontaine, D. J. Geisler, X. Cai, and S. J. B. Yoo, "Demonstration of free space coherent optical communication using integrated silicon photonic orbital angular momentum devices," *Opt. Exp.*, vol. 20, no. 9, pp. 9396–9402, Apr. 2012.

[6] L. W. Luo, N. Ophir, C. P. Chen, L. H. Gabrielli, C. B. Poitras, K. Bergman, and M. Lipson, "WDM-compatible mode-division multiplexing on a silicon chip," *Nat. Commun.*, vol. 5, pp. 1–7, Jan. 2014.

[7] J. Wang, S. He, and D. Dai, "On-chip silicon 8-channel hybrid (de)multiplexer enabling simultaneous mode- and polarization-division-multiplexing," *Laser Photon. Rev.*, vol. 8, no. 2, pp. L18–L22, Mar. 2014.

[8] F. Morichetti, S. Grillanda, and A. Melloni, "Breakthroughs in photonics 2013: Toward feedback-controlled integrated photonics," *IEEE Photon. J.*, vol. 6, no. 2, pp. 1–6, Apr. 2014.

[9] D. A. B. Miller, "Self-configuring universal linear optical component," *Photon. Res.*, vol. 1, no. 1, pp. 1–15, Jun. 2013.

[10] F. Morichetti, S. Grillanda, M. Carminati, G. Ferrari, M. Sampietro, M. J. Strain, M. Sorel, and A. Melloni, "Non-invasive on-chip light observation by contactless waveguide conductivity monitoring," *IEEE J. Sel. Top. Quantum Electron.*, vol. 20, no. 4, pp. 292–301, Jul. 2014.

[11] S. Grillanda, M. Carminati, F. Morichetti, P. Ciccarella, A. Annoni, G. Ferrari, M. Strain, M. Sorel, M. Sampietro, and A. Melloni, "Non-invasive monitoring and control in silicon photonics using CMOS integrated electronics," *Optica*, vol. 1, no. 3, pp. 129–136, Sep. 2014.

[12] M. Gnan, S. Thoms, D. S. Macintyre, R. M. De la Rue, and M. Sorel, "Fabrication of low-loss photonic wires in silicon-on-insulator using hydrogen silsesquioxane electron-beam resist," *Electron. Lett.*, vol. 44, no. 2, pp. 115–116, Jan. 2008.

[13] T. Baehr-Jones, M. Hochberg, and A. Scherer, "Photodetection in silicon beyond the band edge with surface states," *Opt. Exp.*, vol. 16, no. 3, pp. 1659–1668, Jan. 2008.